Topological Spin Phases of Trapped Rydberg Excitons in Cu_2O

A. N. Poddubny* and M. M. Glazov†
Ioffe Institute, St. Petersburg 194021, Russia

(Received 4 April 2019; revised manuscript received 24 June 2019; published 16 September 2019)

We theoretically study Rydberg excitons in one-dimensional chains of traps in Cu_2O coupled via the van der Waals interaction. The triplet of optically active p-shell states acts as an effective spin 1, and the interactions between the excitons are strongly spin dependent. We predict that the system has the topological Haldane phase with the diluted antiferromagnetic order, long-range string correlations, and finite excitation gap. We also analyze the effect of the trap geometry and interactions anisotropy on the Rydberg exciton spin states and demonstrate that a rich spin phase diagram can be realized showing high tunability of the Rydberg exciton platform.

DOI: 10.1103/PhysRevLett.123.126801

Introduction.—Rydberg states of matter draw a lot of interest nowadays. Strongly excited atoms are macroscopic quantum objects highly susceptible to external fields that serve for benchtop studies of quantum effects at a large scale [1]. Enhanced polarizability of Rydberg atoms results in efficient interactions, making them a platform of choice for quantum simulations [2–4].

An exciton, the Coulomb interaction correlated electron-hole pair, emerges in semiconductors when an electron is optically promoted from the filled valence to an empty conduction band. It is a direct analog of the hydrogen atom [5]. The perfection of the natural cuprous oxide crystals has not only made it possible to discover large-radius excitons in semiconductors [6], but has also lead to a recent breakthrough: the demonstration of stable highly excited excitonic Rydberg states with the principal quantum number n up to 25 [7]. Importantly, the spatial extension of the $n = 25$ exciton in Cu_2O reaches 1 μm bridging nanoscale and microscale physics in a semiconductor environment. In contrast with Rydberg atoms, excitons exist in the crystalline environment, which manifests itself not only in quantitative differences of the binding energy and exciton radii, but also in different selection rules for optical transitions [8–10] making p-shell excitons with the orbital angular momentum 1 active in single-photon processes, unusual fine structure of the energy spectrum [11], as well as broken symmetries [12,13]. All this provides flexibility to control the excitonic states by light.

Even more profound consequences of the nonzero orbital angular momentum are expected in exciton-exciton interactions in cuprous oxide [14]. Just like for atoms, the interactions are of paramount importance for Rydberg excitons [7] owing to their large radii. By now, the interactions are scarcely studied. However, according to the recent theoretical predictions [14], the coupling between the excitonic states crucially depends on the mutual orientations of their angular momenta.

Similarly to atomic physics, the interaction effects are expected to be the strongest in ensembles of localized Rydberg excitons. Here, we demonstrate that even in a one-dimensional chain of trapped Rydberg excitons in Cu_2O the ground state corresponds to a topologically nontrivial spin order—the Haldane phase [15]—with diluted antiferromagnetic order and a gapped spectrum of elementary excitations. Such a topological phase is inherent to integer spin, in particular spin-1, chains with antiferromagnetic coupling. The hallmarks of the Haldane phase are the nontrivial edge states behaving akin to spin-1/2 fermions as well as the presence of the hidden long-range "string" order despite the apparent lack of distant spin-spin correlations [16].

The concepts of topology are at the heart of modern condensed matter and high-energy physics as topologically nontrivial properties are largely unaffected by external perturbations and depend on the fundamental properties of system's Hamiltonian. For example, the protection of edge states in the quantum Hall effect regime [17–20] and in topological insulators allows one to realize low-dissipation electron transport [21] and the spin-edge states in Haldane chains are promising for quantum technologies [22]. The quest for topologically nontrivial phases of matter is also going on mainly due to the shortage of experimental test systems. For example, despite numerous theoretical proposals [23], so far the Haldane phase has been only probed by the neutron scattering [24] or heat conductivity measurements [25,26] in anisotropic magnetic materials. The topological effects are now being studied for non-interacting [27–30] and interacting exciton polaritons [31,32]. However, this research is fundamentally different, being focused on the topological edge excitations and solitons in the driven-dissipative condensate, rather than on a many-body exciton ground state with a topologically nontrivial spin structure we propose here.

 © 2019 American Physical Society

Thus, the Rydberg excitons provide a highly desirable tabletop solid state platform with direct optical access to individual excitons for both fundamental studies of hidden symmetries and topological orders and prospective quantum simulations [23,33–37].

Chain of Rydberg excitons.—We consider Rydberg excitons confined in a one-dimensional (1D) periodic array of traps, see Fig. 1. The traps for excitons could be created either optically utilizing the ac Stark shift of excitons in the structured light waves, similar to the optical lattices of cold atoms [38], or in a tailored semiconductor environment, where the band gap energy can be controlled by applying a strain or external electrostatic potential [39]. It is assumed that each trap is occupied by a single exciton, that is in a p-shell state with the angular momentum of the envelope function being equal to 1. For simplicity, we neglect here exciton internal spin degrees of freedom, i.e., the spins of electrons and holes, and the spin-orbit interaction. We introduce the pseudovector angular momentum operator $\boldsymbol{S}_j = (S_j^x, S_j^y, S_j^z)$ for jth trap. Hereafter, we use the term spin to denote $\boldsymbol{S}_j$ for brevity, and z is the chain axis. We assume that the traps are sufficiently well separated; thus the excitons in neighboring traps are coupled to each other by the van der Waals interaction only. The effects of the exchange interaction require an overlap of excitonic wave functions and can be neglected in the considered chain under the conditions $a_n \ll d \ll R$, where a_n is the radius of the excited exciton state and d is the trap size [40–42]. In this situation the interaction Hamiltonian is also independent of the trap size and geometry in the leading order in $d/R \ll 1$. Owing to a strong R^{-6} decay of the potential with the distance between the traps R, it is sufficient to consider the nearest-neighbor approximation. The Hamiltonian of the chain has the form $\mathcal{H} = \sum_{j=1}^{N-1} \mathcal{H}_{\rm bond}(\boldsymbol{S}_j, \boldsymbol{S}_{j+1})$, where N is the number of traps equal to the number of excitons in the system, $\mathcal{H}_{\rm bond}$ is the neighbors' coupling Hamiltonian. The system has a rotational symmetry around the z axis. Thus, $\mathcal{H}_{\rm bond}$ is characterized by seven real constants [43] $c_0, \ldots, c_6$ and can be presented as

$$\begin{aligned}\mathcal{H}_{\rm bond}(\boldsymbol{S}_1, \boldsymbol{S}_2) = {} & c_0 + c_1 S_1^z S_2^z + c_2 (S_1^x S_2^x + S_1^y S_2^y) \\ & + c_3 (S_1^z S_2^z)^2 + c_4 (S_1^x S_2^x + S_1^y S_2^y)^2 \\ & + c_5 [S_1^z S_2^z (S_1^x S_2^x + S_1^y S_2^y) + \text{H.c.}] \\ & + c_6 (S_1^x S_2^y - S_1^y S_2^x)^2. \end{aligned} \tag{1}$$

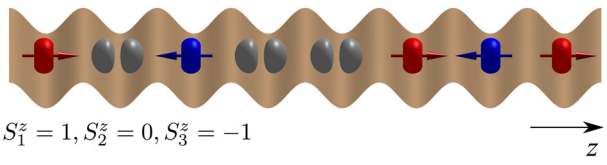

FIG. 1. Schematics of the diluted antiferromagnetic state formed from p-shell Rydberg excitons in an array of traps.

The microscopic calculation in Ref. [14] confirms that all seven parameters are significant. Specifically, for the exciton with principal quantum numbers $n = 12, \ldots, 25$ one has [14]

$$\begin{aligned} & c_0 = -5.58\mathcal{E}, \quad c_1 = 9.53\mathcal{E}, \quad c_2 = -8.97\mathcal{E}, \quad c_3 = 1.27\mathcal{E}, \\ & c_4 = 6.59\mathcal{E}, \quad c_5 = -3.18\mathcal{E}, \quad c_6 = 5.04\mathcal{E}, \end{aligned} \tag{2}$$

where the common factor $\mathcal{E}$ is $10^{-4} n^{11}\ \hbar\,\mathrm{s}^{-1} \times \mu\mathrm{m}^6/R^6$. The Hamiltonian is invariant to the change of parameters $c_2 \to -c_2$, $c_5 \to -c_5$ which corresponds to reflection $z \to -z$ for every second spin. Importantly, the spin-spin coupling is mainly antiferromagnetic ($c_1 > 0$) and strongly anisotropic. For the exciton separation on the order of a micrometer and the principal quantum number $n \sim 20$ the typical energy scales are in the 10 μeV range making it feasible to observe the many-body phases at the mK temperatures; see Supplemental Material [44] for details.

Since the Rydberg blockade prevents two particles from being close to each other [1,2,7], in what follows we neglect the exciton tunneling between the traps and disregard the polariton effect [54]. The interplay of the interactions and tunneling can enrich the spin phases in bosonic systems [55]. The trap, however, can affect the angular momentum state of the exciton giving rise to the anisotropic single particle contributions [44]. We first disregard the anisotropy and discuss its effect at the end of the Letter.

Ground and excited state energies.—The chain Hamiltonian cannot be diagonalized analytically for $N > 3$. Instead, we first solved numerically for the lowest energy states in small finite chains ($N \le 14$) with the periodic boundary conditions [56]. The results of calculation are shown in Fig. 2. The ground state energy, shown in the inset, quickly converges to the value of $E_0 \approx -3.51N\mathcal{E}$. The ground state is nondegenerate for periodic boundary conditions and has the total spin $\sum_j S_j^z = 0$. The system is gapped, with the excitation gap slowly decreasing with the size. The lowest excited state has zero total spin projection and the excitation energy $E_g \gtrsim 1.1\mathcal{E}$ (red open symbols in Fig. 2). The states with $\sum_j S_j^z = \pm 1$ have significantly larger excitation energies $E_g' \gtrsim 6\mathcal{E}$ (blue filled symbols). In order to reveal the structure of the excited states we have compared the results of exact diagonalization with those obtained from the single-magnon variational approach [57,58]. Namely, we used the trial wave function

$$\psi_k \propto \frac{1}{\sqrt{N}} \sum_{j=1}^{N} e^{ikj} S_j^z \psi_0, \tag{3}$$

for the first excited state, where ψ_0 is the numerically calculated ground state, and the wave vector has been set to $k = \pi$ [44]. The variational energy is close to the exact one, which indicates that the excited state is well described by the ansatz equation (3). The large overlap (about 0.99) between Eq. (3) and the lowest excited state has been also confirmed

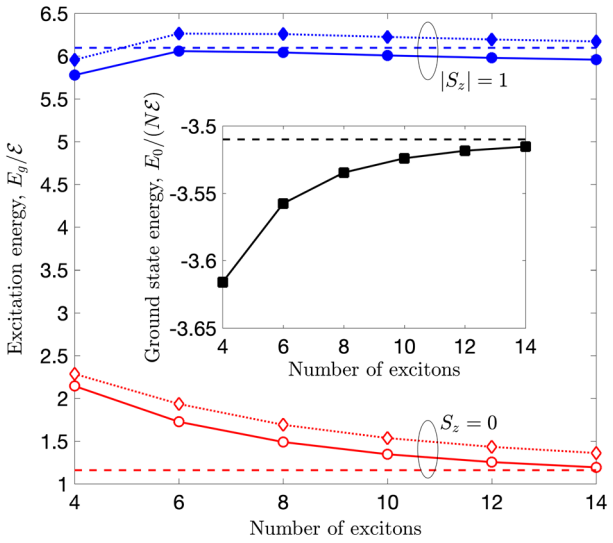

FIG. 2. Ground and excited state energies in spin chains of different lengths with the periodic boundary conditions. Open symbols correspond to the lowest excited state with the total spin projection $\sum S_j^z = 0$, filled symbols correspond to the double-degenerate states with $\sum S_j^z = \pm 1$. Squares indicate results of direct numerical calculation, diamonds correspond to the energies of the variational states Eqs. (3) and (4) with $k = \pi$ and 0, respectively. Dashed lines are the variational results obtained for the infinite system. The inset shows the ground state energy per bond, $E_0/(N\mathcal{E})$, for the finite chain (symbols) and the infinite chain (dashed line).

numerically. The lowest excited states with the ± 1 total spin projection being degenerate due to the time-reversal symmetry were sought in the form

$$\psi_k \propto \frac{1}{\sqrt{N}} \sum_{j=1}^{N} e^{ikj} [\mu_1 S_j^z + \mu_2 S_j^z (S_j^x \pm i S_j^y)] \psi_0, \qquad (4)$$

with $k = 0$ [44] and $\mu_{1,2}$ being the variational coefficients. The energy of this trial state is close to the exact numerical result as well, cf. blue circles and diamonds in Fig. 2.

In addition to the exact diagonalization of small finite chains we have also employed the infinite time-evolving block decimation (ITEBD) approach [59–61]. The advantage of this numerical technique is that it is capable to directly address infinite chains. It is based on the representation of the ground state ψ_0 in the matrix-product form [62]

$$\psi_{i_1 i_2 i_3 \ldots} \propto M^{i_1}_{\alpha_1 \alpha_2} M^{i_2}_{\alpha_2 \alpha_3} M^{i_3}_{\alpha_3 \alpha_4} \ldots, \qquad (5)$$

where M is a certain third rank tensor, indices $i_j = 0, +1, -1$ label the projections of the spin j, and $\alpha_j = 1, \ldots, \chi$ are auxiliary indices. If the spins were independent, one could use $\chi = 1$, so that the α indices are irrelevant, $M^i_{\alpha_j \alpha_{j+1}} \to M^i$ and the state Eq. (5) would reduce to a simple product state. For $\chi > 1$ the state Eq. (5) can describe quantum entanglement (i.e., correlations) between the spins. The ITEBD approach enables high-accuracy description of arbitrary gapped noncritical 1D systems with local Hamiltonians [62,63] at relatively low computational cost. In our case, the convergence of energy better than 1% has been already reached for the rank $\chi \lesssim 20$.

The ITEBD results for the infinite system are shown in Fig. 2 by dashed horizontal lines. The energies of both ground and excited states agree well with the corresponding results for the finite chains. The excited state energies in the infinite system were estimated using the same variational approximation Eqs. (3) and (4) with ψ_0 being now the ground state found from ITEBD. We have also calculated the dispersion of excitations $E_g(k)$ in the single magnon approximation [44]. In agreement with the analysis of the finite system, the spin-0 magnon branch is indeed gapped with the minimum at the edge of the Brillouin zone, $k = \pi$, while the magnons with ± 1 spin projection have the minimum energy at $k = 0$.

Spin structure of the ground state.—Now we proceed to the analysis of the spin-spin correlations in the ground state. The calculation has been performed for the infinite chain using the ITEBD technique. The results are shown in Fig. 3. We start with the analysis of the pair spin-spin correlations depending on the spin-spin distance j. The calculation demonstrates the presence of short-range antiferromagnetic Néel order,

$$C_{\text{Néel}}(j) \equiv (-1)^j \langle S_0^z S_j^z \rangle. \qquad (6)$$

At large distances the spin correlations Eq. (6) vanish, as illustrated by the red dashed curve in Fig. 3 showing the exponential decay with the correlation length ≈7. Hence, based only on the analysis of local spin-spin correlations one could conclude that the considered spin phase has no

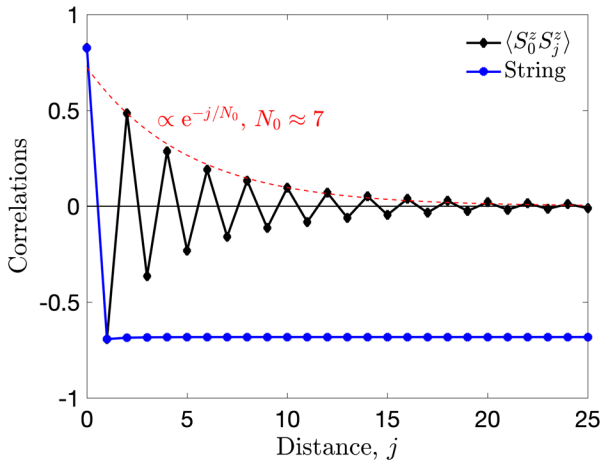

FIG. 3. Spin-spin correlator $(-1)^j C_{\text{Néel}(j)}$ and string correlator for ground state of the infinite chain of Rydberg excitons, Eqs. (6) and (7).

long-range order. However, this is not the case. Our main result is that the infinite chains of Rydberg excitons do possess a long-range string order, characterized by the nonvanishing correlator [16]

$$C_{\text{string}}(j) = \langle S_0^z e^{i\pi(S_1^z+S_2^z+\ldots S_{j-1}^z)} S_j^z \rangle, \tag{7}$$

blue circles in Fig. 3. The presence of the nonlocal order parameter $C_{\text{string}}(j)$ can be interpreted as a result of spontaneous breaking of a certain $\mathbb{Z}_2 \times \mathbb{Z}_2$ symmetry, hidden in the system [64]. Such string order in the absence of Néel order has been first revealed in the Affleck-Kennedy-Lieb-Tasaki model with $\mathcal{H}_{\text{bond}} = \boldsymbol{S}_1 \cdot \boldsymbol{S}_2 + (\boldsymbol{S}_1 \cdot \boldsymbol{S}_2)^2/3$ [65,66]. The Affleck-Kennedy-Lieb-Tasaki model is exactly solvable by the matrix-product state Eq. (5) with certain rank-2 matrices [64]. Similar ansatz has allowed us to obtain the ground state energy with $E_0 = -3.49N\mathcal{E}$ [44] analytically, which is very close to the numerically obtained value of $E_0 = -3.51N\mathcal{E}$ shown in the inset of Fig. 2. The simultaneous presence of the string order and the absence of the Néel order, along with the presence of the nondegenerate gapped ground state are the clear fingerprints of the Haldane phase of spin-1 excitons [15,67]. Physically, this indicates so-called diluted antiferromagnetism where the wave function of the ground state ψ_0 can be represented as a superposition of basic functions in the form

$$|\ldots, 0\ldots, 0, 1, -1, 0, \ldots, 1, -1, 1, 0, \ldots\rangle,$$

where the significant part of excitons is in the $S^z = 0$ state, and the spins $S^z = \pm 1$ can occur only in pairs, i.e., $+1, -1$ or $-1, +1$, while the pairs $+1, +1$ or $-1, -1$ are forbidden. Thus, the string correlator singles out "diluted antiferromagnetic order," where neighboring spins are always opposite with the possible arbitrary number of zeros in between. The fact that the pair $+1, -1$ or $-1, +1$ can occur at any arbitrary place of the chain is related to the formation of the topological Haldane phase in our system. Such a diluted antiferromagnetic state is schematically illustrated in Fig. 1. Experimentally, spin states and spin correlations can be measured by the polarization of light emitted by the excitons.

The smoking gun evidence for the Haldane phase is the presence of edge states in a finite chain with open boundary conditions behaving as spin-1/2 fermions [16,34]. Our direct numerical calculations for $N \leq 14$ exciton chains have indeed confirmed that, in the case of open boundary conditions, the ground state corresponds to four closely lying levels corresponding to the combinations of edge spins-1/2 slightly split due to the finite chain size [44].

Phase diagram.—The Haldane phase is a robust generic feature of 1D spin-1 chains with antiferromagnetic nearest-neighbor interaction. For instance, it is known to exist in isotropic bilinear-biquadratic spin chains with $\mathcal{H}_{\text{bond}} = -\cos\theta \boldsymbol{S}_1 \cdot \boldsymbol{S}_2 + \sin\theta (\boldsymbol{S}_1 \cdot \boldsymbol{S}_2)^2$ in a wide range of angles around $\theta = \pi$, including the spin-1 anisotropic Heisenberg model [68]. In order to demonstrate that the formation of the Haldane phase for the Rydberg excitons is not a coincidence, we have analyzed the structure of the ground state depending on the anisotropy of the trap shape and on the sign of the coupling, either ferromagnetic or antiferromagnetic. The trap anisotropy has been described by adding the single particle terms $\mathcal{H}_1 = D\sum_j [(S_j^z)^2 - 2/3]$ to the Hamiltonian [44]. The coupling anisotropy was described by an additional term $\delta c_1 S_1^z S_2^z$ in the bond Hamiltonian equation (1). The structure of the ground state was determined by the comparison of the spin-spin and string correlations at large distances. The results of this analysis are summarized in Fig. 4, and the correlation functions are given in the Supplemental Material [44].

We start the discussion of the phase diagram Fig. 4 with the role of the coupling term $\delta c_1 S_1^z S_2^z$. Clearly, for large positive δc_1 the spin-spin interaction becomes antiferromagnetic, $\langle S_1^z S_2^z \rangle = -1$, while for negative δc_1 the system is driven in the ferromagnetic phase with $\langle S_1^z S_2^z \rangle = 1$. The anisotropic ferromagnetic order, indicated by the pink area in Fig. 4, is characterized by the long-range spin-spin correlations with $\langle S_1^z S_2^z \rangle < 1$. The Haldane phase is realized in the antiferromagnetic regime in the wide range of the trap anisotropy parameter D provided that it is not large negative.

The impact of the anisotropy has also a transparent interpretation: Large positive values of D favor the $S^z = 0$ ground state first facilitating the formation of the diluted antiferromagnetic state and, ultimately, the nonmagnetic state with $S_j^z \equiv 0$ at each site. Similarly to the spin-1 Heisenberg model, even slight anisotropy $D < 0$ switches the system into the antiferromagnetic state [69]. Large negative values of D push down $S^z = \pm 1$ states rendering

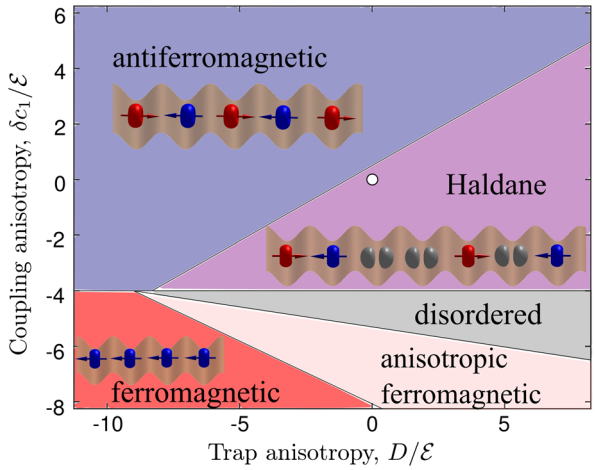

FIG. 4. Phase diagram of the ground state depending on the trap anisotropy and the spin-spin coupling anisotropy. Insets illustrate the typical spin configurations. The white circle indicates the parameters of Ref. [14] ($D = \delta c_1 = 0$).

the exciton chain to the set of 1/2-pseudospins and suppressing the Haldane phase.

We are grateful to M. Aßmann, M. Bayer, T. Pohl, M. A. Semina, and V. Walther for fruitful discussions. M. M. G. is grateful to RSF Project No. 17-12-01265 for partial support. A. N. P. acknowledges support of the Russian President Grant No. MD-5791.2018 and the Foundation for the Advancement of Theoretical Physics and Mathematics "BASIS."

*poddubny@coherent.ioffe.ru
†glazov@coherent.ioffe.ru

[1] T. Gallagher, *Rydberg Atoms*, Cambridge Monographs on Atomic Physics (Cambridge University Press, Cambridge, England, 2005).
[2] M. Saffman, T. G. Walker, and K. Mølmer, Quantum information with Rydberg atoms, Rev. Mod. Phys. **82**, 2313 (2010).
[3] H. Bernien, S. Schwartz, A. Keesling, H. Levine, A. Omran, H. Pichler, S. Choi, A. S. Zibrov, M. Endres, M. Greiner, V. Vuletić, and M. D. Lukin, Probing many-body dynamics on a 51-atom quantum simulator, Nature (London) **551**, 579 (2017).
[4] A. Keesling, A. Omran, H. Levine, H. Bernien, H. Pichler, S. Choi, R. Samajdar, S. Schwartz, P. Silvi, S. Sachdev, P. Zoller, M. Endres, M. Greiner, V. Vuletić, and M. D. Lukin, Quantum Kibble–Zurek mechanism and critical dynamics on a programmable Rydberg simulator, Nature (London) **568**, 207 (2019).
[5] *Excitons*, edited by E. I. Rashba and M. D. Sturge (North-Holland Publishing Company, Amsterdam, 1982).
[6] E. F. Gross and N. A. Karrjew, Light absorption by cuprous oxide crystal in infrared and visible part of the spectrum, Dokl. Akad. Nauk SSSR **84**, 471 (1952).
[7] T. Kazimierczuk, D. Fröhlich, S. Scheel, H. Stolz, and M. Bayer, Giant Rydberg excitons in the copper oxide Cu_2O, Nature (London) **514**, 343 (2014).
[8] S. Zielińska-Raczyńska, G. Czajkowski, and D. Ziemkiewicz, Optical properties of Rydberg excitons and polaritons, Phys. Rev. B **93**, 075206 (2016).
[9] J. Heckötter, M. Freitag, D. Fröhlich, M. Aßmann, M. Bayer, M. A. Semina, and M. M. Glazov, Scaling laws of Rydberg excitons, Phys. Rev. B **96**, 125142 (2017).
[10] M. A. Semina, Fine structure of Rydberg excitons in cuprous oxide, Phys. Solid State **60**, 1527 (2018).
[11] J. Thewes, J. Heckötter, T. Kazimierczuk, M. Aßmann, D. Fröhlich, M. Bayer, M. A. Semina, and M. M. Glazov, Observation of High Angular Momentum Excitons in Cuprous Oxide, Phys. Rev. Lett. **115**, 027402 (2015).
[12] M. Aßmann, J. Thewes, D. Fröhlich, and M. Bayer, Quantum chaos and breaking of all anti-unitary symmetries in Rydberg excitons, Nat. Mater. **15**, 741 (2016).
[13] F. Schweiner, J. Main, and G. Wunner, Magnetoexcitons Break Antiunitary Symmetries, Phys. Rev. Lett. **118**, 046401 (2017).
[14] V. Walther, S. O. Krüger, S. Scheel, and T. Pohl, Interactions between Rydberg excitons in Cu_2O, Phys. Rev. B **98**, 165201 (2018).
[15] F. D. M. Haldane, Nonlinear Field Theory of Large-Spin Heisenberg Antiferromagnets: Semiclassically Quantized Solitons of the One-Dimensional Easy-Axis Néel State, Phys. Rev. Lett. **50**, 1153 (1983).
[16] M. den Nijs and K. Rommelse, Preroughening transitions in crystal surfaces and valence-bond phases in quantum spin chains, Phys. Rev. B **40**, 4709 (1989).
[17] R. B. Laughlin, Quantized Hall conductivity in two dimensions, Phys. Rev. B **23**, 5632 (1981).
[18] F. D. M. Haldane, Model for a Quantum Hall Effect Without Landau Levels: Condensed-Matter Realization of the "Parity Anomaly", Phys. Rev. Lett. **61**, 2015 (1988).
[19] G. Jotzu, M. Messer, R. Desbuquois, M. Lebrat, T. Uehlinger, D. Greif, and T. Esslinger, Experimental realization of the topological Haldane model with ultracold fermions, Nature (London) **515**, 237 (2014).
[20] G. Salerno, M. Di Liberto, C. Menotti, and I. Carusotto, Topological two-body bound states in the interacting Haldane model, Phys. Rev. A **97**, 013637 (2018).
[21] B. A. Bernevig, T. L. Hughes, and S.-C. Zhang, Quantum spin Hall effect and topological phase transition in HgTe quantum wells, Science **314**, 1757 (2006).
[22] B. Jaworowski and P. Hawrylak, Quantum bits with macroscopic topologically protected states in semiconductor devices, Appl. Sci. **9**, 474 (2019).
[23] J. Xu, Q. Gu, and E. J. Mueller, Realizing the Haldane Phase with Bosons in Optical Lattices, Phys. Rev. Lett. **120**, 085301 (2018).
[24] W. Lu, J. Tuchendler, M. von Ortenberg, and J. P. Renard, Direct Observation of the Haldane Gap in NENP by Far-Infrared Spectroscopy in High Magnetic Fields, Phys. Rev. Lett. **67**, 3716 (1991).
[25] A. V. Sologubenko, T. Lorenz, J. A. Mydosh, A. Rosch, K. C. Shortsleeves, and M. M. Turnbull, Field-Dependent Thermal Transport in the Haldane Chain Compound NENP, Phys. Rev. Lett. **100**, 137202 (2008).
[26] T. Kawamata, Y. Miyajima, N. Takahashi, T. Noji, and Y. Koike, Large thermal conductivity due to spins in the Haldane gap system Y_2BaNiO_5, J. Magn. Magn. Mater. **310**, 1212 (2007).
[27] A. V. Nalitov, D. D. Solnyshkov, and G. Malpuech, Polariton $\mathbb{Z}$ Topological Insulator, Phys. Rev. Lett. **114**, 116401 (2015).
[28] T. Karzig, C.-E. Bardyn, N. H. Lindner, and G. Refael, Topological Polaritons, Phys. Rev. X **5**, 031001 (2015).
[29] F. Wu, T. Lovorn, and A. H. MacDonald, Topological Exciton Bands in Moiré Heterojunctions, Phys. Rev. Lett. **118**, 147401 (2017).
[30] S. Klembt, T. H. Harder, O. A. Egorov, K. Winkler, R. Ge, M. A. Bandres, M. Emmerling, L. Worschech, T. C. H. Liew, M. Segev, C. Schneider, and S. Höfling, Exciton-polariton topological insulator, Nature (London) **562**, 552 (2018).
[31] C.-E. Bardyn, T. Karzig, G. Refael, and T. C. H. Liew, Chiral Bogoliubov excitations in nonlinear bosonic systems, Phys. Rev. B **93**, 020502(R) (2016).
[32] D. D. Solnyshkov, O. Bleu, and G. Malpuech, Topological optical isolator based on polariton graphene, Appl. Phys. Lett. **112**, 031106 (2018).

[33] A. Imambekov, M. Lukin, and E. Demler, Spin-exchange interactions of spin-one bosons in optical lattices: Singlet, nematic, and dimerized phases, Phys. Rev. A **68**, 063602 (2003).

[34] F. Pollmann, E. Berg, A. M. Turner, and M. Oshikawa, Symmetry protection of topological phases in one-dimensional quantum spin systems, Phys. Rev. B **85**, 075125 (2012).

[35] C. Nayak, S. H. Simon, A. Stern, M. Freedman, and S. Das Sarma, Non-Abelian anyons and topological quantum computation, Rev. Mod. Phys. **80**, 1083 (2008).

[36] C.-K. Chiu, J. C. Y. Teo, A. P. Schnyder, and S. Ryu, Classification of topological quantum matter with symmetries, Rev. Mod. Phys. **88**, 035005 (2016).

[37] R. Samajdar, S. Choi, H. Pichler, M. D. Lukin, and S. Sachdev, Numerical study of the chiral $\mathbb{Z}_3$ quantum phase transition in one spatial dimension, Phys. Rev. A **98**, 023614 (2018).

[38] I. Bloch, Ultracold quantum gases in optical lattices, Nat. Phys. **1**, 23 (2005).

[39] D. P. Trauernicht, J. P. Wolfe, and A. Mysyrowicz, Thermodynamics of strain-confined paraexcitons in Cu_2O, Phys. Rev. B **34**, 2561 (1986).

[40] C. Ciuti, V. Savona, C. Piermarocchi, A. Quattropani, and P. Schwendimann, Role of the exchange of carriers in elastic exciton-exciton scattering in quantum wells, Phys. Rev. B **58**, 7926 (1998).

[41] S. B.-T de-Leon and B. Laikhtman, Exciton-exciton interactions in quantum wells: Optical properties and energy and spin relaxation, Phys. Rev. B **63**, 125306 (2001).

[42] M. Combescot, O. Betbeder-Matibet, and F. Dubin, The many-body physics of composite bosons, Phys. Rep. **463**, 215 (2008).

[43] A. Klümper, A. Schadschneider, and J. Zittartz, Matrix product ground states for one-dimensional spin-1 quantum antiferromagnets, Europhys. Lett. **24**, 293 (1993).

[44] See Supplemental Material at http://link.aps.org/supplemental/10.1103/PhysRevLett.123.126801 for contains details of additional calculations of exciton energy spectra and spin-spin correlations, which includes Refs. [45–53].

[45] J. Haegeman, S. Michalakis, B. Nachtergaele, T. J. Osborne, N. Schuch, and F. Verstraete, Elementary Excitations in Gapped Quantum Spin Systems, Phys. Rev. Lett. **111**, 080401 (2013).

[46] J. Haegeman, T. J. Osborne, and F. Verstraete, Post-matrix product state methods: To tangent space and beyond, Phys. Rev. B **88**, 075133 (2013).

[47] V. Zauner, D. Draxler, L. Vanderstraeten, M. Degroote, J. Haegeman, M. M. Rams, V. Stojevic, N. Schuch, and F. Verstraete, Transfer matrices and excitations with matrix product states, New J. Phys. **17**, 053002 (2015).

[48] L. Landau and E. Lifshitz, *Quantum Mechanics: Non-Relativistic Theory* (Butterworth-Heinemann, Oxford, 1977).

[49] F. Schweiner, J. Main, M. Feldmaier, G. Wunner, and C. Uihlein, Impact of the valence band structure of Cu_2O on excitonic spectra, Phys. Rev. B **93**, 195203 (2016).

[50] W. Que, Excitons is quantum dots with parabolic confinement, Phys. Rev. B **45**, 11036 (1992).

[51] M. A. Semina, R. A. Sergeev, and R. A. Suris, Localization of electron-hole complexes at fluctuations of interfaces of quantum dots, Semiconductors **40**, 1338 (2006).

[52] S. K. Lyo, Energy transfer of excitons between quantum wells separated by a wide barrier, Phys. Rev. B **62**, 13641 (2000).

[53] D. Fröhlich, A. Kulik, B. Uebbing, V. Langer, H. Stolz, and W. von der Osten, Propagation beats of quadrupole polaritons in Cu_2O, Phys. Status Solidi (b) **173**, 31 (1992).

[54] M. Takahata, K. Tanaka, and N. Naka, Nonlocal optical response of weakly confined excitons in Cu_2O mesoscopic films, Phys. Rev. B **97**, 205305 (2018).

[55] A. M. Belemuk, N. M. Chtchelkatchev, A. V. Mikheyenkov, and K. I. Kugel, Magnetic phase diagram and quantum phase transitions in a two-species boson model, Phys. Rev. B **96**, 094435 (2017).

[56] We considered only chains with even N, since the odd number is incompatible with antiferromagnetic order, resulting in slower numerical convergence.

[57] D. P. Arovas, A. Auerbach, and F. D. M. Haldane, Extended Heisenberg Models of Antiferromagnetism: Analogies to the Fractional Quantum Hall Effect, Phys. Rev. Lett. **60**, 531 (1988).

[58] E. Bartel, A. Schadschneider, and J. Zittartz, Excitations of anisotropic spin-1 chains with matrix product ground state, Eur. Phys. J. B **31**, 209 (2003).

[59] G. Vidal, Efficient Classical Simulation of Slightly Entangled Quantum Computations, Phys. Rev. Lett. **91**, 147902 (2003).

[60] G. Vidal, Efficient Simulation of One-Dimensional Quantum Many-Body Systems, Phys. Rev. Lett. **93**, 040502 (2004).

[61] G. Vidal, Classical Simulation of Infinite-Size Quantum Lattice Systems in One Spatial Dimension, Phys. Rev. Lett. **98**, 070201 (2007).

[62] R. Orús, A practical introduction to tensor networks: Matrix product states and projected entangled pair states, Ann. Phys. (Amsterdam) **349**, 117 (2014).

[63] G. Vidal, J. I. Latorre, E. Rico, and A. Kitaev, Entanglement in Quantum Critical Phenomena, Phys. Rev. Lett. **90**, 227902 (2003).

[64] T. Kennedy and H. Tasaki, Hidden symmetry breaking and the Haldane phase in $S = 1$ quantum spin chains, Commun. Math. Phys. **147**, 431 (1992).

[65] I. Affleck, T. Kennedy, E. H. Lieb, and H. Tasaki, Valence bond ground states in isotropic quantum antiferromagnets, Commun. Math. Phys. **115**, 477 (1988).

[66] T. Kennedy and H. Tasaki, Hidden $Z_2 \times Z_2$ symmetry breaking in Haldane-gap antiferromagnets, Phys. Rev. B **45**, 304 (1992).

[67] F. Haldane, Continuum dynamics of the 1-D Heisenberg antiferromagnet: Identification with the O(3) nonlinear sigma model, Phys. Lett. **93A**, 464 (1983).

[68] U. Schollwöck, J. Richter, D. J. Farnell, and R. F. Bishop, *Quantum Magnetism* (Springer, Berlin, 2008), Vol. 645.

[69] W. Chen, K. Hida, and B. C. Sanctuary, Ground-state phase diagram of $S = 1$ XXZ chains with uniaxial single-ion-type anisotropy, Phys. Rev. B **67**, 104401 (2003).